

Electric Charge in Presence of Fixed Monopole-Antimonopole Pair

Niloufar Barghi-Janyar and Amir H. Fatollahi *

*Department of Physics, Alzahra University,
P. O. Box 19938, Tehran 91167, Iran*

* `fath@alzahra.ac.ir`

Abstract

The dynamics of an electric charge e in presence of a fixed monopole pair $\pm g$ is considered. Depending on the ratio of the angular momentum to eg/c , the effective potential may consist a minimum valley between the poles or a finite depth well. In the classical limit the charge may be bound to the poles inside the minimum valley or well. In the quantum theory, due to the finite barrier between the minimum and the potential at infinity, only approximate or quasi bound-states are possible. Based on the Rayleigh-Ritz variational method the energy and eigen-functions are obtained. The implications on the proposed confining mechanism based on the dual picture of the so-called Meissner effect is pointed.

Keywords: Magnetic monopoles

PACS No.: 14.80.Hv

1 Introduction

The magnetic field by a single magnetic monopole of strength g at origin is given by

$$\mathbf{B} = g \mathbf{r}/r^3 \quad (1)$$

This can be obtained by means of $\mathbf{B} = \nabla \times \mathbf{A}$ with [1]

$$\mathbf{A} = g \frac{\mathbf{r} \times \hat{\mathbf{n}}}{r(r - \mathbf{r} \cdot \hat{\mathbf{n}})} \quad (2)$$

Except along the half-line $\mathbf{r} = \alpha \hat{\mathbf{n}}$ with $\alpha \geq 0$, the above vector potential is regular [1]. In fact the singular line acts as an intensive field inside the ultra-thin solenoid to cancel the outward flow by the monopole; the so-called Dirac string [2]. By the choice $\hat{\mathbf{n}} = \hat{\mathbf{z}}$ (2) reduces to the well known expression [3]

$$\mathbf{A} = g \frac{1 + \cos \theta}{r \sin \theta} \hat{\phi} \quad (3)$$

Demanding the wave-function of the electric charge e in presence of the monopole to be single-valued, the quantization condition follows [4, 5]:

$$e g/c = q \hbar/2, \quad q = 0, \pm 1, \pm 2, \dots \quad (4)$$

It is known that a monopole and an electric charge do not make bound-state [6]. The bound-state problem of two dyons (states with both electric and magnetic charges) is considered in [1], where the exact energy eigen-values are obtained for cases that the dyonic bound-states are possible.

In the present work the problem of the dynamics of an electric charge in presence of a fixed monopole-antimonopole pair is considered. In the Hamiltonian formulation of the system the effective potential in the ρz -plane describes the nature of possible bound-states. Accordingly it is found that, depending on the ratio of angular momentum and the combination of charges in (4), the effective potential may consist minimum valley or well accompanied by a saddle-point, or no extrema at all. In the classical regime, when the potential has a minimum the bound motion of the electric charge is possible. In the quantum theory, as the minimum is apart from the tail $V \rightarrow 0$ at infinity with finite height barrier, the formation of true bound-state is not possible. It is known that, due to the tunneling effect through a barrier of finite height and width, only the so-called quasi bound-states are possible. However, for the case with large barrier height these states may treated approximately as bound-states.

The results by the present study can directly be used in the dual picture, in which the dynamics of a monopole is considered in the presence of two fixed opposite electric charges. Apart from pure theoretical curiosity, the problem in dual picture can shed light on the confinement mechanism in gauge theories based on the dual picture of the so-called Meissner effect in type-II superconductors. It is known that the electric charges make a circulating motion around the thin magnetic fluxes inside the superconductors, hence the name of vortex for these thin magnetic fluxes. In fact the circulating motion of electric charges around the magnetic fluxes prevent the magnetic fields to spread inside the superconductor, leading to the

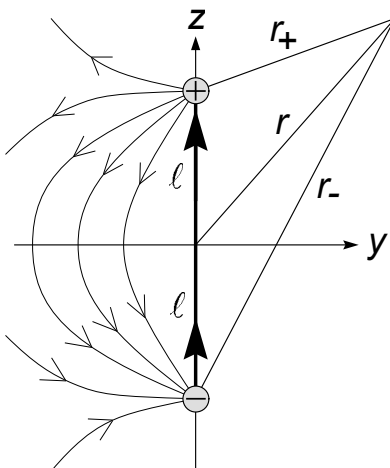


Figure 1: The setup with monopole pairs. The only singular part is the segment between the poles. The thick arrow exhibits the direction of intense field flux inside the Dirac string.

confinement of the hypothetical monopole and anti-monopole pair inserted inside the sample. In the proposed confinement mechanism, it is the motion of the monopoles that prevents the spreading of the electric fluxes, leading to the confining phase of the theory [7–9].

The organization of the rest of paper is as follows. In Sec. 2 the setup of the system is presented together with the Hamiltonian formulation of the classical system. The nature of dynamics is discussed based on the effective potential in the ρz -plane, together with the bound-state and the scattering problems. In Sec. 3 the quantum dynamics is formulated and developed. Based on the variational Rayleigh-Ritz method the energy eigen-values are obtained for the cases that the approximate bound-states are expected. In Sec. 4 the concluding remarks and discussions are presented.

2 Classical Dynamics

The magnetic field by a monopole $+g$ and antimonopole $-g$ on z -axis, respectively at $z = \ell$ and $z = -\ell$, is given by:

$$\mathbf{B} = g \left(\frac{\mathbf{r}_+}{r_+^3} - \frac{\mathbf{r}_-}{r_-^3} \right) \quad (5)$$

in which (see Fig. 1)

$$\begin{aligned} \mathbf{r}_\pm &= \mathbf{r} \mp \ell \hat{\mathbf{z}} \\ &= \rho \hat{\boldsymbol{\rho}} + (z \mp \ell) \hat{\mathbf{z}} \\ r_\pm &= \sqrt{\rho^2 + (z \mp \ell)^2} \end{aligned} \quad (6)$$

The Lorentz equation of motion of the electric charge e with mass μ , $\mu \ddot{\mathbf{r}} = e \dot{\mathbf{r}} \times \mathbf{B}/c$, in

the cylindrical coordinates (ρ, ϕ, z) , leads to

$$\mu(\ddot{\rho} - \rho\dot{\phi}^2) = \frac{eg}{c}\rho\dot{\phi}\left(\frac{z-\ell}{r_+^3} - \frac{z+\ell}{r_-^3}\right) \quad (7)$$

$$\mu(\rho\ddot{\phi} + 2\dot{\rho}\dot{\phi}) = \frac{eg}{c}\left(\frac{\rho\dot{z} - \dot{\rho}(z-\ell)}{r_+^3} - \frac{\rho\dot{z} - \dot{\rho}(z+\ell)}{r_-^3}\right) \quad (8)$$

$$\mu\ddot{z} = \frac{eg}{c}\rho^2\dot{\phi}\left(\frac{1}{r_+^3} - \frac{1}{r_-^3}\right) \quad (9)$$

Among others, one possible solution corresponds to motion along the curve with almost fixed ϕ defined by

$$\mathbf{v} \times \mathbf{B} \approx 0 \quad \rightarrow \quad \frac{dz}{d\rho} \approx \frac{B_z}{B_\rho} \quad (10)$$

It is easy to check that the uniform circular motion in the xy -plane around the z -axis also satisfies the above equations:

$$\rho \equiv \rho_0, \quad \phi = \omega t, \quad z \equiv 0 \quad (11)$$

provided that

$$\omega = \frac{2eg\ell}{\mu c(\rho_0^2 + \ell^2)^{3/2}} \quad (12)$$

Simple force analysis shows that stable circular motion against small perturbations can be expected. Later in the Hamiltonian formulation the condition for the stable solutions corresponding to two solutions in above are discussed in detail.

2.1 Effective Potential

The Lagrangian formulation of the problem is possible. By the polar angles θ_\pm for monopoles (see Fig. 1), with the choice (3) and using $r_- \sin \theta_- = r_+ \sin \theta_+ = \rho$, we have

$$\begin{aligned} \mathbf{A} &= g \left(\frac{1 + \cos \theta_-}{r_- \sin \theta_-} - \frac{1 + \cos \theta_+}{r_+ \sin \theta_+} \right) \hat{\phi} \\ &= \frac{g}{\rho} (\cos \theta_- - \cos \theta_+) \hat{\phi} \end{aligned} \quad (13)$$

The form chosen in above is such that the only singular part is on z -axis in $-\ell \leq z \leq \ell$. The Lagrangian $L = \frac{1}{2}\mu\dot{\mathbf{r}}^2 + \frac{e}{c}\dot{\mathbf{r}} \cdot \mathbf{A}$, using $v_\phi = \rho\dot{\phi}$, then comes to the form

$$L = \frac{1}{2}\mu(\dot{\rho}^2 + \rho^2\dot{\phi}^2 + \dot{z}^2) + \frac{eg}{c}\dot{\phi}(\cos \theta_- - \cos \theta_+) \quad (14)$$

The canonical momenta by the above are then

$$\begin{aligned} p_\rho &= \mu\dot{\rho}, & p_z &= \mu\dot{z}, \\ p_\phi &= \mu\rho^2\dot{\phi} + \frac{eg}{c}(\cos \theta_- - \cos \theta_+) \end{aligned} \quad (15)$$

As the ϕ coordinate is absent in the Lagrangian its canonical momentum p_ϕ is conserved. The Hamiltonian of the system is easily obtained to be

$$H = \frac{p_\rho^2 + p_z^2}{2\mu} + V_{\text{eff}}(\rho, z) \quad (16)$$

in which the effective potential in the ρz -plane is

$$V_{\text{eff}}(\rho, z) = \frac{1}{2\mu} [F(\rho, z)]^2 \quad (17)$$

with

$$F(\rho, z) = \frac{1}{\rho} \left(p_\phi - \frac{eg}{c} (\cos \theta_- - \cos \theta_+) \right) \quad (18)$$

$$= \frac{1}{\rho} \left(p_\phi - \frac{eg}{c} \left(\frac{z + \ell}{r_-} - \frac{z - \ell}{r_+} \right) \right) \quad (19)$$

The last expression presents the explicit ρ and z dependences. Evidently $V_{\text{eff}} \geq 0$, with the zero as the absolute minimum. The extrema of the potential are obtained by either conditions:

$$\text{Cond. (1) :} \quad F(\rho, z) = 0, \quad (20)$$

$$\text{Cond. (2) :} \quad \partial_\rho F(\rho, z) = 0, \quad \partial_z F(\rho, z) = 0 \quad (21)$$

The first condition defines the zero valley $V = 0$ along the below curve in the ρz -plane:

$$\cos \theta_- - \cos \theta_+ = \frac{z + \ell}{r_-} - \frac{z - \ell}{r_+} = \frac{c p_\phi}{eg} \quad (22)$$

It is easy to check that differentiating d/dt of above leads to (10), and so (22) corresponds to the motion along the curve between two poles with fixed ϕ coordinate. Using the fact that $0 \leq (\cos \theta_- - \cos \theta_+) \leq 2$, the first condition is satisfied only when

$$0 \leq \frac{c p_\phi}{eg} \leq 2 \quad (23)$$

The second condition (21) defines the other types of extrema, not necessarily a minimum one. The condition (21) leads to $z = 0$ together with (see Appendix)

$$\frac{c p_\phi}{eg} = 2 \cos \theta_0 (1 + \sin^2 \theta_0), \quad \rho_0 = \ell \tan \theta_0 \quad (24)$$

by which the equilibrium distance ρ_0 in the $z = 0$ plane is given. The plot of the right-hand side of (24) is presented in Fig. 2. The above has solution for $0 \leq \theta_0 \leq \pi/2$ when

$$0 \leq \frac{c p_\phi}{eg} \leq \frac{8\sqrt{2}}{3\sqrt{3}} \simeq 2.18 \quad (25)$$

The second derivative determines the nature of the extrema, by defining $\rho_c = \ell/\sqrt{2}$, for which we have

$$\partial_\rho^2 F = \frac{4eg\ell}{c r_0^5 \rho_0} (\rho_c^2 - \rho_0^2) \quad (26)$$

$$\partial_z^2 F = \frac{6eg\ell}{c r_0^5} \rho_0, \quad \partial_\rho \partial_z F = 0 \quad (27)$$

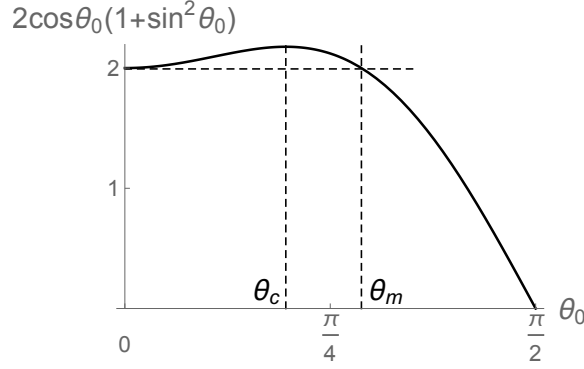


Figure 2: The plot of right-hand side of (24), with $\theta_c = \sin^{-1}\frac{1}{\sqrt{3}}$ and $\theta_m = \cos^{-1}\left(\frac{-1+\sqrt{5}}{2}\right)$.

By above for $\rho_0 < \rho_c$ we have a minimum, otherwise it is a saddle-point extremum (note $\partial_z^2 F > 0$). The case with $cp_\phi/(eg) = 2$ is special. In this case the extrema occur at

$$\text{minimum at } \theta_0 = 0 : \quad \rho_0 = 0, \quad -\ell \leq z \leq \ell \quad (28)$$

$$\text{saddle-point at } \theta_0 = \theta_m : \quad \rho_0 = \sqrt{\frac{2}{\sqrt{5}-1}} \ell, \quad z = 0 \quad (29)$$

with $\theta_m = \cos^{-1}\frac{-1+\sqrt{5}}{2} \simeq 0.9046$ rad (see Appendix). In summary, we have the following about the extrema of the effective potential:

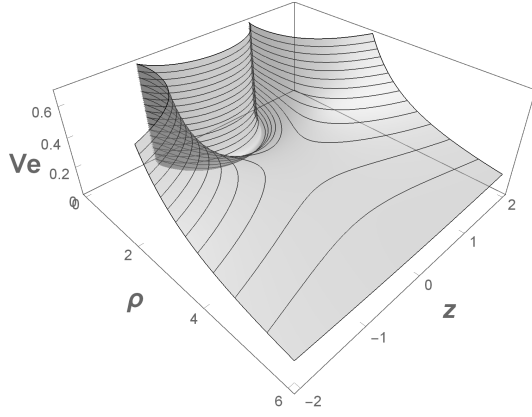
- $0 \leq \frac{cp_\phi}{eg} \leq 2$: minimum valley along curve $F(\rho, z) = 0$ between two poles accompanied by an outer saddle-point $\rho_0 > \rho_c$ and $z = 0$ by the single solution of (24) (the solution with $\theta_0 > \theta_m$ in Fig 2). A sample plot of potential is presented in Fig. 3a.
- $2 \leq \frac{cp_\phi}{eg} \leq \frac{8\sqrt{2}}{3\sqrt{3}}$: an inner local minimum well at $\rho_{01} < \rho_c$ and $z = 0$ accompanied by an outer saddle-point at $\rho_{02} > \rho_c$ and $z = 0$ both by the double solutions of (24) (two solutions with $0 < \theta_0 < \theta_m$ in Fig 2). A sample plot of potential is presented in Fig. 3b. The motion with constant ρ_0 is then a circular one with the constant angular velocity

$$\dot{\phi} = \frac{1}{\mu \rho_0^2} \left(p_\phi - 2 \frac{eg\ell}{cr_0} \right) = 2 \frac{eg\ell}{\mu cr_0^3} \quad (30)$$

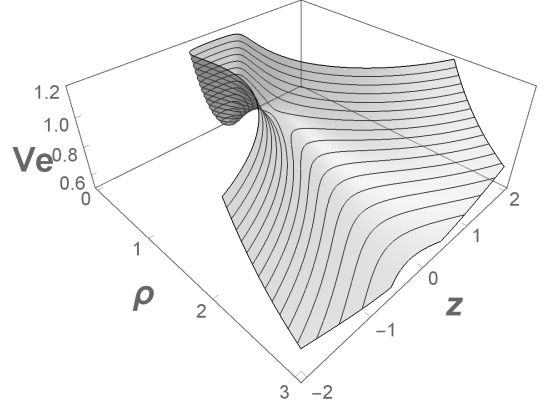
with $r_0 = \sqrt{\rho_0^2 + \ell^2}$, which is exactly (12) by the equations of motion.

- $\frac{cp_\phi}{eg} \geq \frac{8\sqrt{2}}{3\sqrt{3}}$: no local extrema

In the classical dynamics we can have stable motions about the minima. As examples in Fig. 4 slightly perturbed motions about the two cases in above are presented. However as will see shortly, the situation is different in the quantum theory, in which a barrier with finite-width can not have real bound-states due to the tunneling effect.

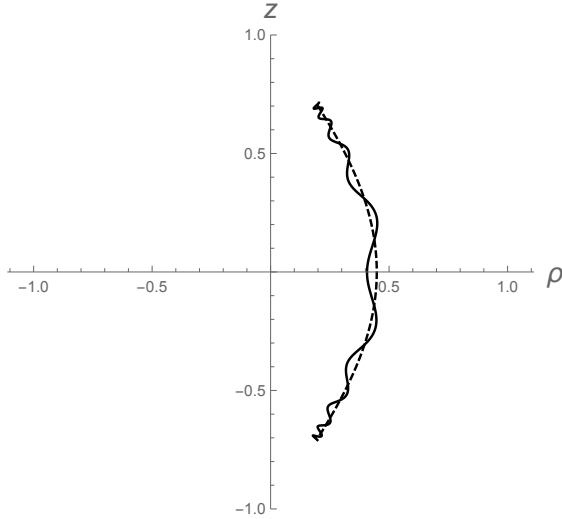


(a) $p_\phi = 3$, $eg/c = 2.4$ and $\ell = 1$

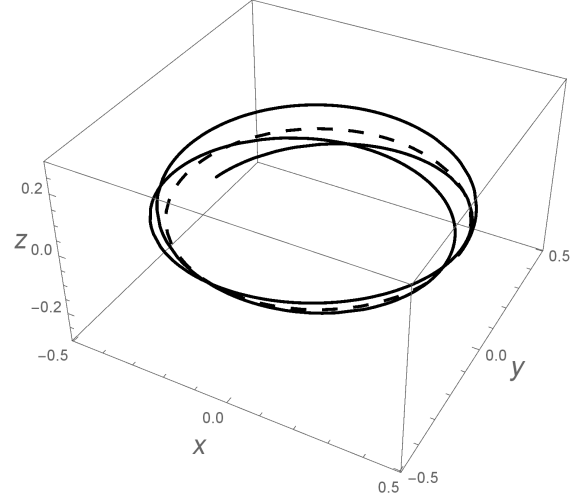


(b) $p_\phi = 3$, $eg/c = 1.44$, and $\ell = 1$

Figure 3



(a) The ρz -projection of the 3D helical motion (solid-line) around the curve $F(\rho, z) = 0$ (dashed-line). The plot is by values: $\mu = 1$, $\ell = 1$, $eg/c = 2.8$, $cp_\phi/eg = 1.825$, $\rho_0 = 0.204$, $\dot{\rho}_0 = 0.0204$, $z_0 = 0.714$, $\dot{z}_0 = -0.142$, $\phi_0 = 0$, $\dot{\phi}_0 = 5$.



(b) The circular motion (dashed-line) and perturbed (solid-line) motion around the z axis. The plot is by values: $\mu = 1$, $\ell = 1$, $eg/c = 1$, $cp_\phi/eg = 2.12$, $\rho_0 = 0.42$, $\dot{\rho}_0 = 0.05$, $z_0 = 0$, $\dot{z}_0 = 0.06$, $\phi_0 = 0$, $\dot{\phi}_0 = 1.57$

Figure 4

2.2 Scattering

The above analysis on the effective potential can be used to study the scattering processes as well. The problem of scattering of an electric charge by a single monopole is studied in [10–12]. In the system by one monopole the total angular momentum \mathbf{J} of charge and electromagnetic fields is conserved, by which it can be shown that the motion of electric

charge is entirely on a cone with the monopole at its apex [10]. This fact lets to eliminate the coordinate parallel to the axes of cone, leading to an exact solution for the motion projected on the plane perpendicular to the axes of cone [10]. The relation between the scattering angle θ and the impact parameter b in the reduced two dimensional problem can be obtained analytically [10], which can be inserted in the classical relation [13]:

$$\frac{d\sigma}{d\Omega} = \frac{b}{\sin\theta} \left| \frac{db}{d\theta} \right| \quad (31)$$

For the small impact parameters, where the cone is narrower, the scattering angle θ oscillates about the scattering angle π (backward direction) [10]. The cross section goes to infinity whenever the oscillating function passes $\theta = \pi$, leading to the so-called backward glory phenomena [13]. Also due to the vanishing of $d\theta/db$ at the extrema of the oscillating function $\theta(b)$, the cross section also diverges at some other impact parameters, leading to the so-called rainbow effect [10].

In the present problem the rotational symmetry is explicitly broken to an axial one around the axes passing the monopoles, here is taken to be the z -axes. As the consequence, only the z component of the total angular momentum, here denoted by p_ϕ in (15), is conserved. Similar to the case with one single monopole, the axial symmetry around z direction suggests to project the motion on the xy -plane, however in this case the motion is not confined to a cone and numerical solutions are to be developed. By the analysis based on the effective potential we already know that for $0 \leq \frac{cp_\phi}{eg} \leq 2.18$ the potential has an attractive part, beyond it the potential is totally repulsive. It is known that when the potential has an attractive part the so-called quasi-stable orbiting paths may develop infinite values for the polar angle [13]. Further one should expect vanishing deflection angle for a finite value of impact parameter for which the attractive part of potential cancels out the effect of the repulsive part, leading to the forward glory effect [13]. Interestingly both of these effects are present for the scattering from a monopole pair. For the incoming charges with $\mathbf{v}_0 = -v_0 \hat{\mathbf{x}}$ in the xy -plane, for which $p_\phi = \mu b v_0$, the results of the numerical solutions as the paths in the xy -plane for different impact parameters are plotted in Fig. 5. The paths clearly show both the repulsive and the attracting effects on the incoming charges. In fact for appropriate values of p_ϕ together with sufficient value of $E_0 = \mu v_0^2/2$ to overcome the maximum of the potential hump (see Figs. 3 & 4), the charges are affected by the attractive part too. The values of the polar angles of outgoing charges for different impact parameters are plotted in Fig. 6a. The result is quite in accordance with expectations from the scattering theory by potentials with attractive part [13]. All the incoming angles have the initial polar angle $\phi_0 = 0$, and so those with $\phi_\infty \rightarrow \pm\pi$ are to be considered as undeflected ones. As usual the large impact parameters $b \rightarrow \pm\infty$ lead to the undeflected ones at two ends of the plot in Fig. 6a. The values of polar angles by three values of impact parameters are to be recognized. First is about the impact parameter at which the deflection angle is π (polar angle $\phi_\infty = 0$). This impact parameter is denoted by b_1 in Fig. 6a, at which the cross section diverges and is known as the backward glory effect. The second is about the impact parameter at which the repulsive and attractive parts in potential cancel out the effect of each other, leading to zero deflection ($\phi_\infty = \pi$). This impact parameter is denoted by b_2 in Fig. 6a, at which the

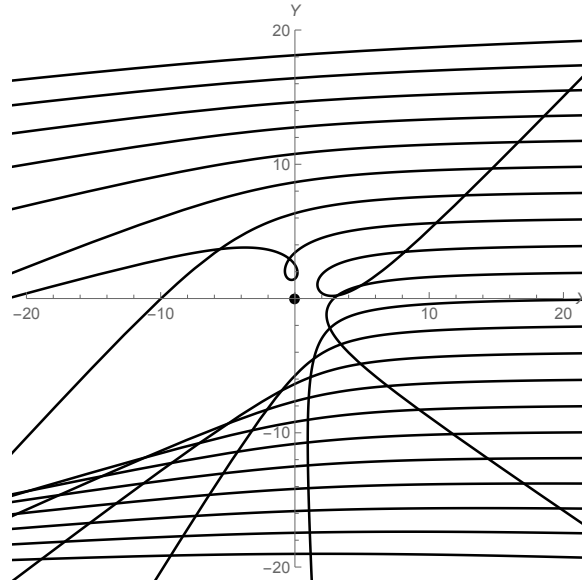
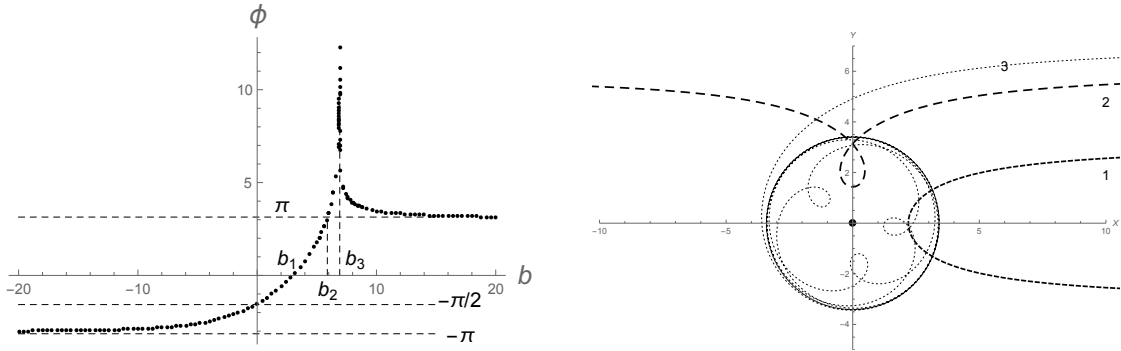


Figure 5: The paths in the xy -plane for different impact parameters for values $\mu = 1$, $\ell = 1$, $eg/c = 2.8$, and $v_0 = 1.2$.

cross section is diverging and is known as the forward glory effect. The third is the impact parameter at which the energy is equal to the potential hump and the charge makes a quasi-stable orbiting path, leading to infinite polar angle. This impact parameter is b_3 in Fig. 6a. The paths corresponding to the impact parameters b_1 , b_2 and b_3 are plotted in Fig. 6b as paths 1, 2 and 3, respectively.



(a) The polar angle versus the impact parameter by the numerical solutions for initial values in Fig. 5. The introduced values are $b_1 = 2.97$, $b_2 = 5.88$, and $b_3 = 6.92$.

(b) The three paths 1, 2 and 3 for impact parameters b_1 , b_2 , and b_3 , corresponding to backward, forward and quasi-stable paths, respectively.

Figure 6

3 Quantum Dynamics

The Hamiltonian operator in the cylindrical coordinates takes the form

$$H = -\frac{\hbar^2}{2\mu} \left(\frac{1}{\rho} \frac{\partial}{\partial \rho} \rho \frac{\partial}{\partial \rho} + \frac{\partial^2}{\partial z^2} \right) + \frac{1}{2\mu\rho^2} \left(p_\phi - \frac{eg}{c} \left(\frac{z+\ell}{r_-} - \frac{z-\ell}{r_+} \right) \right)^2 \quad (32)$$

In the quantum theory the quantization conditions read

$$p_\phi = m\hbar, \quad m = 0, \pm 1, \pm 2, \dots \quad (33)$$

$$eg/c = q\hbar/2, \quad q = 0, \pm 1, \pm 2, \dots \quad (34)$$

Replaced by the dimensionless coordinates $\rho \rightarrow \ell\rho$ and $z \rightarrow \ell z$, the Hamiltonian for fixed $p_\phi = m\hbar$ takes the form:

$$H_m = \frac{\hbar^2}{2\mu\ell^2} \left[-\frac{1}{\rho} \frac{\partial}{\partial \rho} \rho \frac{\partial}{\partial \rho} - \frac{\partial^2}{\partial z^2} + \frac{1}{\rho^2} \left(m - \frac{q}{2} \left(\frac{z+1}{r_-} - \frac{z-1}{r_+} \right) \right)^2 \right] \quad (35)$$

in which $\frac{\hbar^2}{2\mu\ell^2}$ has the energy dimension, and we have for the dimensionless distances

$$r_\pm = \sqrt{\rho^2 + (z \mp 1)^2} \quad (36)$$

The Schrodinger equation for fixed $p_\phi = m\hbar$ then might be represented as

$$H_m \Psi_m(\rho, z) = \frac{\hbar}{2\mu\ell^2} E_m \Psi_m(\rho, z) \quad (37)$$

in which E_m is the dimensionless eigen-value of H_m . Since the ℓ -dependence can be factored out, the nature of the eigen-functions is independent of the value of ℓ . It is known that due to the tunneling effect, in presence of a finite height and width barrier a true bound-states do not exist in the quantum theory. In the present problem this simply means that, the charge initially located around the minimum of the potential will eventually tunnel to infinity through the barrier. The irrelevance of the value of ℓ in this respect can be understood simply by the tunneling effect as follows. It is known that the transmission rate T depends on the barrier height ΔV and its width ΔL through the relation $T \simeq \exp\left(-2\sqrt{\frac{2\mu}{\hbar^2} \Delta V \Delta L}\right)$. For the value of the potential at extrema by condition (24) we easily find the finite height:

$$\begin{aligned} V_{\text{eff}} \Big|_{\text{extrema}} &= \frac{2}{\mu} \left(\frac{eg}{c} \right)^2 \frac{\ell^2 \rho_0^2}{r_0^6} \\ &= \frac{2}{\mu} \left(\frac{eg}{c} \right)^2 \frac{1}{\ell^2} \sin^2 \theta_0 \cos^4 \theta_0 \end{aligned} \quad (38)$$

As ℓ is the only parameter of length dimension in the system, we have

$$\left. \begin{aligned} \Delta V &\propto \left(\frac{eg}{c\ell} \right)^2 \\ \Delta L &\propto \ell \end{aligned} \right\} \rightarrow \sqrt{\Delta V \Delta L} \propto eg/c \quad (39)$$

showing that the transition rate is independent of ℓ . Further the above shows that for large enough eg/c the transition rate is so small that the approximate bound-states are expected. By (33) and (34) we have

$$\frac{cp_\phi}{eg} = \frac{2m}{q} \quad (40)$$

Based on the above, one may try to estimate the approximate bound-state spectrum in the large m limit with fixed $2m/q$, for which the electric charge may be considered a bound particle by the monopole pair. Here we use the variational method of Rayleigh-Ritz, in which one starts by a set of basis functions [14]:

$$\chi_1, \chi_2, \dots, \chi_N \quad (41)$$

In general the basis functions are neither orthogonal nor normalized. The variational trial functions are then expanded as

$$\psi = \sum_{i=1}^N c^i \chi_i \quad (42)$$

The aim is to determine the coefficients c^i 's via the variational method to minimize the expectation $\langle H \rangle$. The metric and the Hamiltonian matrix elements are then defined as [14]:

$$H_{ij} = \langle \chi_i | H | \chi_j \rangle = \int d^3x \chi_i^* H \chi_j \quad (43)$$

$$g_{ij} = \langle \chi_i | \chi_j \rangle = \int d^3x \chi_i^* \chi_j \quad (44)$$

Eventually, the eigen-values and eigen-vectors of the Hamiltonian is obtained through the system of equations [14]

$$\sum_{j=1}^N H^i_j c^j = E c^i \quad (45)$$

$$\det(H^i_j - E \delta^i_j) = 0 \quad (46)$$

in which H^i_j is defined by the inverse of the metric g^{ik} [14]:

$$H^i_j = \sum_{k=1}^N g^{ik} H_{kj}, \quad \sum_{k=1}^N g^{ik} g_{kj} = \delta^i_j \quad (47)$$

It can be shown that if one adds the level of truncation from N to $N+1$, the spectrum obtained by (46) would remain unchanged or decreased, as one expects in a variational approach. In the following we use the above method to estimate the energy spectrum of the system.

3.1 $0 < \frac{2m}{q} < 2$: Bound-States in Minimum Valley

Based on (20), the minimum valley is defined by $f(\rho, z) = 0$ with

$$f(\rho, z) = m - \frac{q}{2} \left(\frac{z+1}{r_-} - \frac{z-1}{r_+} \right) \quad (48)$$

Due to square nature of the effective potential (17), the basis in this case are taken to be the combination of the one by Harmonic oscillator, representing oscillations transverse to the valley, plus the standing wave, responsible for oscillations along the valley,

$$\chi_{nn'}(\rho, z) = \exp \left[-\frac{\alpha^2}{2} \left(\frac{f(\rho, z)}{\rho(\rho_{02} - \rho)} \right)^2 \right] H_n(\alpha f(\rho, z)) \sin(n'\theta) \quad (49)$$

$$n = 0, 1, 2, \dots, N, \quad n' = 0, 1, 2, \dots, N'$$

in which H_n is the n -th Hermite polynomial, ρ_{02} is the radius at the saddle-point, and θ is the usual polar angle $\theta = \tan^{-1}(\rho/z)$. The plots of four members of the basis set are presented in Fig. 7. In above α is treated as an extra variational parameter by which we minimize the expectation value. The integration domains in (43) for the dimensionless coordinates are taken to be:

$$0 \leq \rho \leq \rho_{02}, \quad -1 \leq z \leq 1 \quad (50)$$

The denominator $\rho_{02} - \rho$ is inserted in the exponential to ensure the vanishing of the basis functions at saddle-point radius.

Based on (43)-(47), we find convergence in the lowest two levels by changing the level of truncations by the two parameters N and N' from 2 to 5; the number of basis functions are $(5+1)^2 = 36$ for the final trial. For the values:

$$m = 40, \quad q = 50, \quad 2m/q = 1.6 \quad (51)$$

with $V_m = 77.8$ as the value of potential at the saddle-point, the result by the variational method is as following ($\alpha = 0.21$):

$$\psi_{E_1}(\rho, z) \simeq 0.95 \chi_{00} - 0.31 \chi_{02}, \quad E_1 = 31 \quad (52)$$

$$\psi_{E_2}(\rho, z) \simeq 0.89 \chi_{01} - 0.35 \chi_{03}, \quad E_2 = 48 \quad (53)$$

with $E_3 = 65$ which is comparable to the potential at the saddle-point (all energy values are in units $\hbar^2/2\mu\ell^2$). The obtained eigen-functions are plotted in Fig 8.

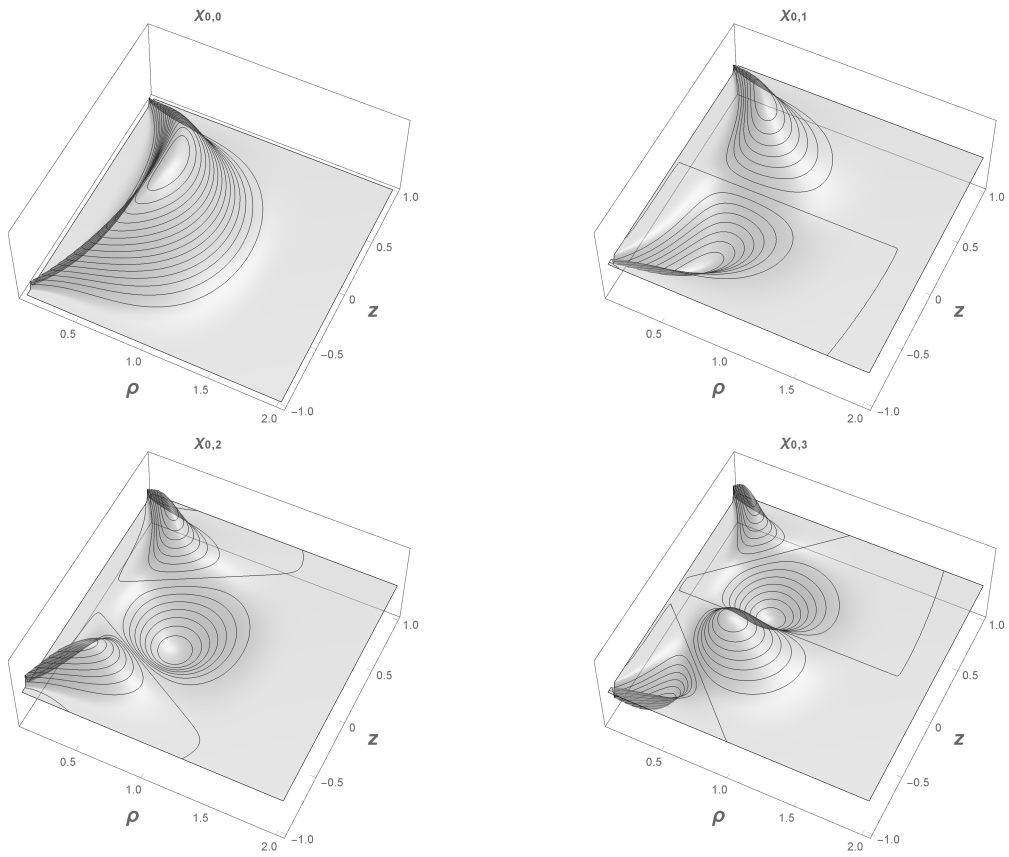


Figure 7: Four members of the trial basis functions by (49) for $m = 40$, $q = 50$ and $\alpha = 0.21$.

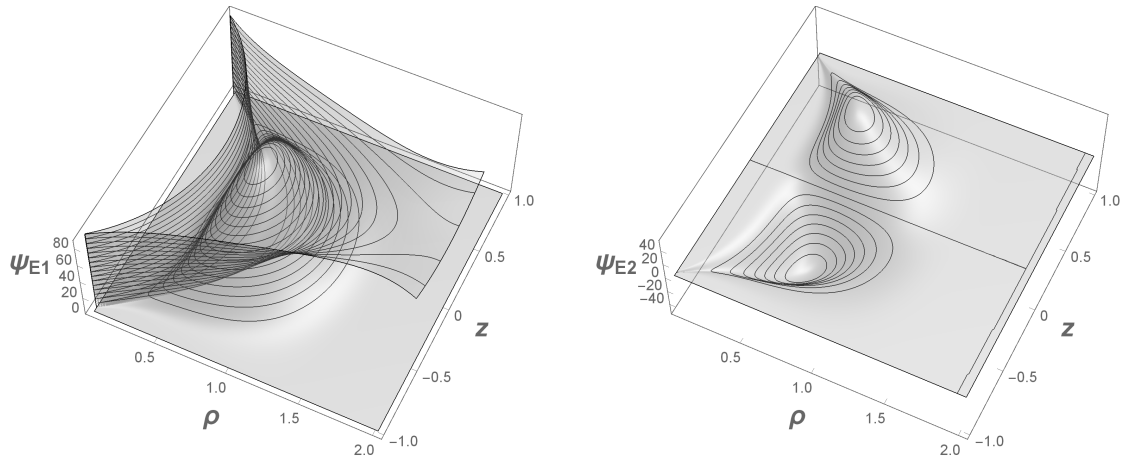


Figure 8: The scaled eigen-functions by (52) and (53). For the ground-state (left) the effective potential is also plotted.

3.2 $2 \leq \frac{2m}{q} \leq \frac{8\sqrt{2}}{3\sqrt{3}}$: Bound-States in Minimum Well

In the case that the minimum makes a well-shape, the trial functions may be developed based on the quadratic expansion of the potential around the minimum. In particular, using

$$\left. \frac{\partial^2 V_{\text{eff}}}{\partial \rho^2} \right|_{\rho_{01},0} = \omega_\rho^2 \quad (54)$$

$$\left. \frac{\partial^2 V_{\text{eff}}}{\partial z^2} \right|_{\rho_{01},0} = \omega_z^2 \quad (55)$$

$$\left. \frac{\partial^2 V_{\text{eff}}}{\partial \rho \partial z} \right|_{\rho_{01},0} = 0 \quad (56)$$

in which ρ_{01} is the minimum point by (24), we may write

$$V_{\text{eff}}(\rho, z) = V_{\text{eff}}(\rho_{01}, 0) + \frac{1}{2}\omega_\rho^2(\rho - \rho_{01})^2 + \frac{1}{2}\omega_z^2 z^2 + \dots \quad (57)$$

Then one simply takes the trial basis functions by the combination of two harmonic oscillators as

$$\begin{aligned} \chi_{nn'}(\rho, z) &= \exp\left[-\frac{\alpha^2}{2}\omega_\rho\left(\frac{\rho - \rho_{01}}{\rho(\rho_{02} - \rho)}\right)^2\right] \text{H}_n(\alpha\sqrt{\omega_\rho}(\rho - \rho_{01})) \\ &\quad \times \exp\left[-\frac{\beta^2}{2}\omega_z z^2\right] \text{H}_{n'}(\beta\sqrt{\omega_z}z) \\ n &= 0, 1, 2, \dots, N, \quad n' = 0, 1, 2, \dots, N' \end{aligned} \quad (58)$$

In Fig. 9 two members of the trial basis functions are plotted. As a specific example the variational method is applied to the case by values

$$m = 52, \quad q = 50, \quad 2m/q = 2.08 \quad (59)$$

with $V_{\text{min}} = 187$ and $V_{\text{sadd.}} = 279$, and

$$\omega_\rho^2 = 2740, \quad \omega_z^2 = 1022 \quad (60)$$

The result by the variational method is as following ($\alpha = 0.21$ and $\beta = 0.91$):

$$\psi_{E_1}(\rho, z) \simeq 0.94 \chi_{00} + 0.33 \chi_{10}, \quad E_1 = 250 \quad (61)$$

with $E_2 = 300$ which is more than the potential at saddle-point, and so can not present a bound-state. The corresponding wave-function is plotted in Fig. 10.

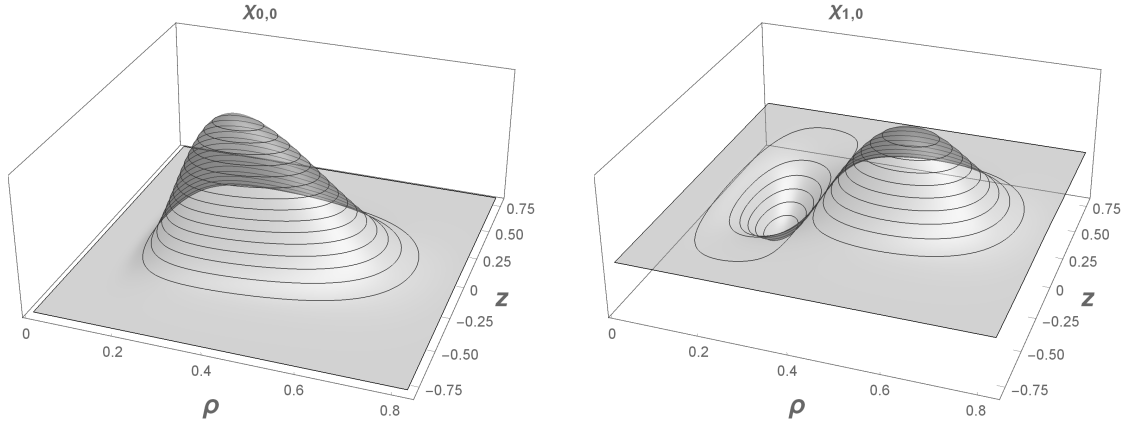


Figure 9: Two members of the trial basis functions by (58) for $m = 52$, $q = 50$, $\alpha = 0.21$ and $\beta = 0.91$.

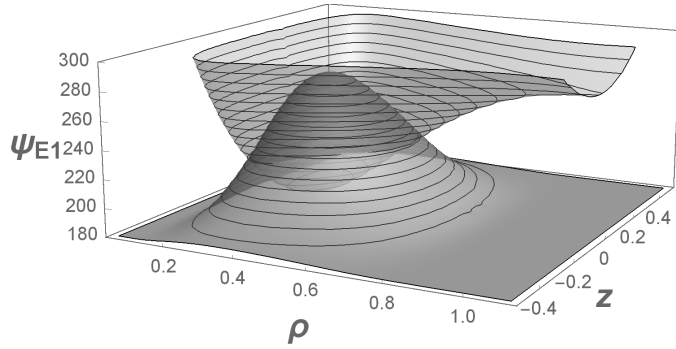


Figure 10: The scaled eigen-function by (61) together with the effective potential.

4 Conclusion and Discussion

The classical and quantum mechanics of the electric charge e in presence of a fixed $\pm g$ pair of magnetic poles is studied. In the Hamiltonian formulation of the system the effective potential $V_{\text{eff}}(\rho, z)$ describes the dynamics. It is found that depending on the ratio of the angular momentum p_ϕ and the combination eg/c the potential may develop extrema. For $0 \leq cp_\phi/eg \leq 2$ the potential consists a zero valley minimum along a curve connecting the poles. For $2 \leq cp_\phi/eg \lesssim 2.18$ the potential consists a finite depth well, and for higher cp_ϕ/eg no extrema is present. The minimum valley or well are separated from $V \rightarrow 0$ tail at infinity by a finite height barrier at a saddle-point. In the classical regime, the case with a minimum valley develop the bound motions along a curve between two poles, and the case with the minimum well may develop the motion around the axis passing two poles. When no extrema in the effective potential naturally no bound-state is expected. In the quantum mechanical setup, due to the tunneling effect through the finite height barrier, the classical bound motions turn to the so-called quasi bound-states. However, for large values of eg/c , for which it is shown that the height of barrier at saddle-point is large, the states may be treated

approximately as true bound-states, for which the energy eigen-values may be evaluated. For these cases by the variational Rayleigh-Ritz method the energy as well as eigen-functions are obtained.

One natural extension of the present problem is to study the statistical mechanics of the electric charges in presence of the monopole pair. In such an extension one may include the dynamics of the fields as well. It is of great importance to study the mutual effect of moving charges and the magnetic fields, and its consequence on the phase structure of the system. This last extension is specially important considering the dual picture of the present problem, in which a gas of monopoles is being considered in presence of two opposite electric charges. As mentioned earlier, according to the confinement mechanism based on the dual picture of the so-called Meissner effect in type-II superconductors, it is the circulating motion of the monopoles that prevents the spreading the electric fluxes, leading to the confinement of the electric charges [7–9]. Based on the results presented here, by considering only the dynamics of charges with given electric field-lines, the system does not develop a bound-state, but only approximate or quasi bound-state. It means that for having a successful explanation of the confinement based on the above mechanism, one has to include the dynamics of fields as well.

A Extrema by $\partial F = 0$

The effective potential has the form

$$V_{\text{eff}}(\rho, z) = \frac{1}{2\mu} \frac{1}{\rho^2} \left(p_\phi - \frac{eg}{c} h(\rho, z) \right)^2 \quad (62)$$

in which

$$h(\rho, z) = \frac{z + \ell}{r_-} - \frac{z - \ell}{r_+} \quad (63)$$

By the condition $\partial_\rho V_{\text{eff}} = 0$ we have

$$h(\rho, z) = 0 \quad (64)$$

$$p_\phi - \frac{eg}{c} \left(h + \rho \frac{\partial h}{\partial \rho} \right) = 0, \quad \text{for } z = 0, \rho = \rho_0 \quad (65)$$

The first in above simply defines the zero-valley minimum. The second leads to

$$p_\phi = 2 \frac{eg}{c} \frac{\ell}{r_0} \left(1 + \frac{\rho_0^2}{r_0^2} \right) \quad (66)$$

with $r_0 = \sqrt{\rho_0^2 + \ell^2}$. The above in terms of the angle $\tan \theta_0 = \rho_0/\ell$ come to the form of (24)

$$\frac{cp_\phi}{eg} = 2 \cos \theta_0 (1 + \sin^2 \theta_0) \quad (67)$$

The right-hand side in above is plotted in Fig. 2, with its extrema coming from vanishing derivative

$$\sin \theta_0 (1 - 3 \sin^2 \theta_0) = 0 \rightarrow \begin{cases} \theta_0 = 0 \\ \theta_c = \sin^{-1} \frac{1}{\sqrt{3}} \end{cases} \quad (68)$$

The second solution in above corresponds the absolute maximum in Fig. 2 with

$$\frac{cp\phi}{eg} = 2 \cos \theta_c (1 + \sin^2 \theta_c) = \frac{8\sqrt{2}}{3\sqrt{3}} \quad (69)$$

The case with $cp\phi/eg = 2$ simply has the below solution corresponding to (29)

$$\cos \theta_m = \frac{-1 + \sqrt{5}}{2} \quad (70)$$

Acknowledgement: This work is supported by the Research Council of the Alzahra University.

References

- [1] D. Zwanziger, “Exactly Solvable Nonrelativistic Model of Particles with both Electric and Magnetic Charges”, *Phys. Rev.* **176** (1968) 1480.
- [2] J.D. Jackson, “Classical Electrodynamics”, John Wiley 2004, sec. 6.12.
- [3] J.J. Sakurai, “Modern Quantum Mechanics”, Addison-Wesley 1994, ch. 2.
- [4] P.A.M. Dirac, “Quantised Singularities in the Electromagnetic Field”, *Proc. Roy. Soc. (London)* **A133** (1931) 60; P.A.M. Dirac, “The Theory of Magnetic Poles”, *Phys. Rev.* **74** (1948) 817.
- [5] K.A. Milton, “Theoretical and Experimental Status of Magnetic Monopoles”, *Rep. Prog. Phys.* **69** (2006) 1637.
- [6] I. Tamm, “Die verallgemeinerten Kugelfunktionen und die Wellenfunktionen eines Elektrons im Feld eines Magnetpoles”, *Z. Physik* **71** (1931) 141.
- [7] Y. Nambu, “Strings, Monopoles, and Gauge Fields”, *Phys. Rev. D* **10** (1974) 4262; “Magnetic and Electric Confinement of Quarks”, *Phys. Rept.* **23** (1976) 250.
- [8] S. Mandelstam, “Vortices and Quark Confinement in Non-Abelian Gauge Theories”, *Phys. Lett. B* **53** (1975) 476; “Vortices and Quark Confinement in Non-Abelian Gauge Theories”, *Phys. Rept.* **23** (1976) 245.
- [9] G. 't Hooft, in *High Energy Physics*, Proceedings of the EPS International Conference, Palermo 1975, ed. A. Zichichi (Editrice Compositori, Bologna, 1976).
- [10] D.G. Boulware, L.S. Brown, R.N. Cahn, S.D. Ellis, and C. Lee, “Scattering on Magnetic Charge”, *Phys. Rev. D* **14** (1976) 2708.
- [11] Y. Kazama, C.N. Yang and A.S. Goldhaber, “Scattering of a Dirac Particle with Charge Ze by a Fixed Magnetic Monopole”, *Phys. Rev. D* **15** (1977) 2287.

- [12] L.F. Urrutia, “Zeroth Order Eikonal Approximation in Relativistic Charged Particle-Monopole Scattering”, *Phys. Rev. D* **18** (1978) 3031.
- [13] H. Goldstein, “Classical Mechanics”, Addison-Wesley 1980, Ed. 2, ch. 3.
- [14] E. Merzbacher, “Quantum Mechanics”, John Wiley 1998, ch. 8.